Vector characterization of a focused terahertz beam

Xinke Wang,[1] Sen Wang,[2] and Yan Zhang[1,3]
[1] Department of Physics, Capital Normal University, XiSanHuan BeiLu No.105, Beijing 100048, China
[2] Department of Physics, Harbin Institute of Technology, Harbin 150001, China

***Abstract*—Vectorial properties of a focused terahertz (THz) beam are measured by using a THz digital holographic imaging system. The THz transverse and longitudinal polarization components around the focal point are obtained utilizing the detection crystals with different crystalline orientations. This imaging technique provides an effective method for presenting the vector diffraction process of the THz wave.**

I. INTRODUCTION

Understanding the vector diffraction properties of electro-magnetic waves is an important basis for both physical optics and applied optics. In this paper, a THz digital holographic imaging system is adopted to coherently probe the vector field of a focused THz beam. The transverse and longitudinal components of the THz field around the focal point are achieved by employing ZnTe crystals with different crystalline orientations, respectively.

II. EXPERIMENTAL SETUP

In this work, a THz digital holographic imaging system shown in Fig. 1 is utilized to characterize the diffraction features of a focused THz beam. The THz radiation is generated by the optical rectification effect. The incident THz beam with the linear polarization (x direction) is focused by a silicon (Si) lens with 25 mm focal length. The probe beam is reflected into a detection crystal by a non-polarization beam splitter (BS). In the crystal, the two dimensional THz field information is loaded on the polarization change of the probe beam. The modulated probe beam is reflected into the imaging module of the system. The THz information is extracted by using the balanced electro-optic detection technique [1]. To measure the vector THz field, the detection crystals with different crystalline orientations are used. When the transverse THz component E_x is measured, a <110> ZnTe is chosen as the detection crystal. When the longitudinal THz component E_z is measured, a <100> ZnTe crystal is selected [2]. A Z-scan measurement is performed by moving the Si lens around the focal point to record the evolution of the focused THz beam.

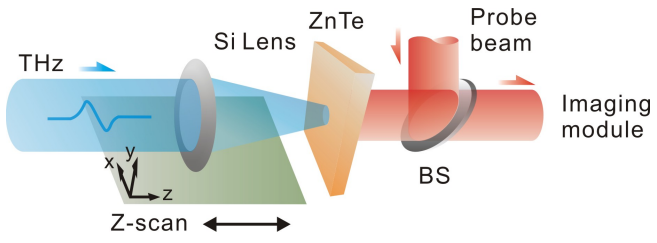

Fig. 1. THz digital holographic imaging system.

III. RESULTS

Figure 2 shows the measured amplitude distributions of the longitudinal component E_z for the 0.7 THz on the planes of z=-10 mm, -5 mm, 0 mm, 5 mm, and 10 mm. A dipole like distribution of E_z can be found, which is caused by the rotational symmetry breaking of the THz polarization after the Si lens. On the focal plane, the minimum value of E_z appears on the optical axis (x=0 mm) and its two maximum values occur around $|x|$=0.4 mm. The corresponding transverse wrapped phase maps of E_z at different scan points are shown in Figs. 2(b). It can be seen that the y-z plane (x=0 mm) is an interface of the phase maps. The phase difference of E_z on two sides of the y-z plane is π, which implies that the propagation directions of E_z are opposite on the two sides of the y-z plane. It can be understand that the minimum of E_z appears on the optical axis is caused by the destructive interference of the fields on the two sides of the y-z plane.

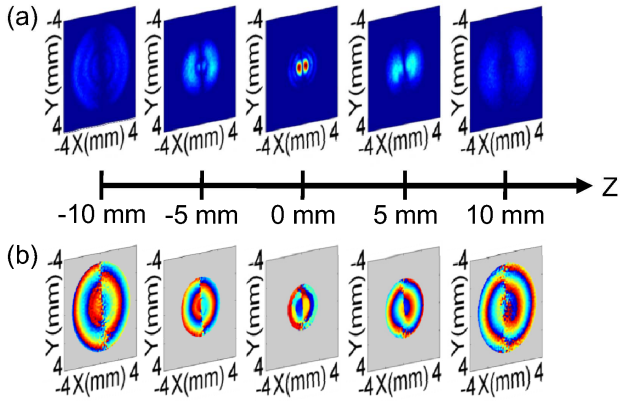

Fig. 2. (a) Measured transverse amplitude distributions of the E_z component on the different observation planes. (b) Corresponding transverse wrapped phase maps.

To further confirm the measurement results, the evolution of E_z during the focusing process is simulated by using the Richards-Wolf formula [3]. Around the focal point, the longitudinal component E_z can be expressed as

$$E_z = -2A\cos\phi\int_0^{\alpha}\sqrt{\cos\theta}\sin^2\theta J_1(kr\sin\theta)\exp(jkz\cos\theta)\,d\theta, \quad (1)$$

where $(r,\ \phi,\ z)$ is the cylindrical coordinate of an observation point, $J_1(kr\sin\theta)$ is the first order Bessel function of the first kind, θ is the angle between the THz beam and the optical axis, $\alpha=\sin^{-1}(\mathrm{NA}/n)$ is the maximum convergence angle of the THz beam and is equivalent to 23° in the experiment, n is the refractive index in the image space and A is a proportionality constant. Fig. 3 shows the amplitude and phase distributions of the simulated E_z on the different observation planes. Apparently, the experimental results are in good agreement with the theoretical expectations, which confirms the accuracy of the experiment.

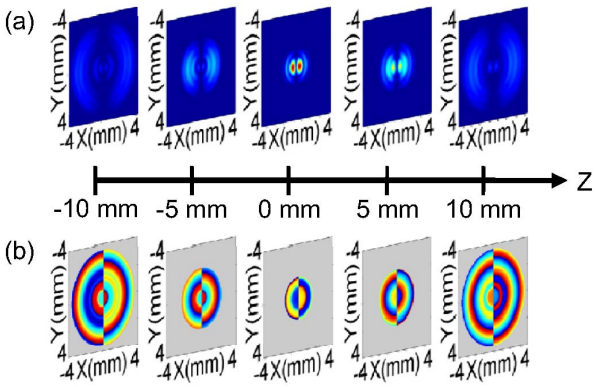

Fig. 3. (a) Simulated transverse amplitude distributions of the E_z component on the different observation planes. (b) Corresponding transverse wrapped phase maps.

In order to analyze the longitudinal component E_z in detail, the transverse and longitudinal normalized profiles of E_z are extracted and plotted in Figs. 4(a) and 4(b). To compare the sizes of E_x and E_z, the amplitude profiles of E_x are also extracted and plotted. It can be seen that the size of the dark region of E_z is about 0.24 mm, which is determined by the distance of two off-axis lobes. In addition, the focal depth of E_z is 6.7 mm, which is approximately the same size as that of E_x.

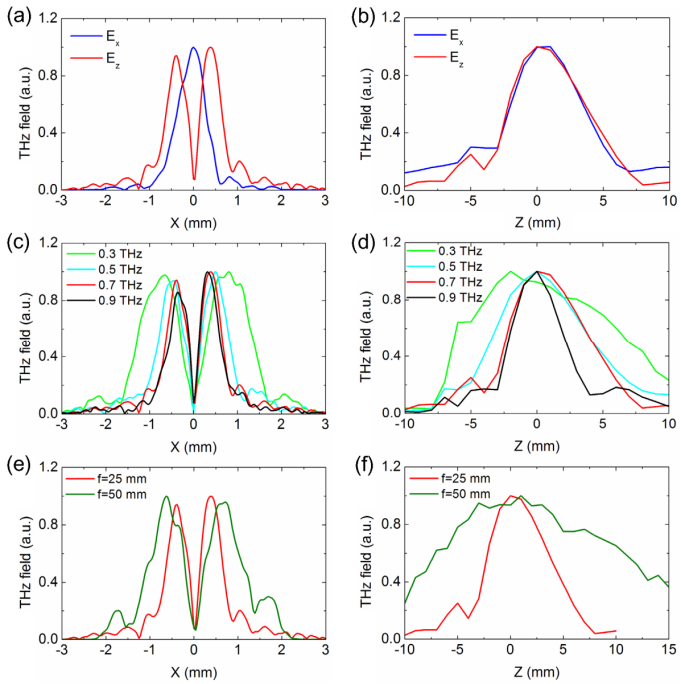

Fig. 4. Normalized transverse (a) and longitudinal (b) amplitude profiles of the E_x and E_z components for 0.7 THz radiation. Normalized transverse (c) and longitudinal (d) amplitude profiles of the E_z components for 0.3 THz, 0.5 THz, 0.7 THz, and 0.9 THz, respectively. Normalized transverse (e) and longitudinal (f) amplitude profiles of the E_z components focused by lenses with 25 mm and 50 mm focal lengths, respectively.

To observe the dispersive properties of E_z, the transverse and longitudinal profiles of 0.3 THz, 0.5 THz, 0.7 THz, and 0.9 THz components are extracted and plotted in Figs. 4(c) and 4(d), respectively. The dark region sizes are 0.55 mm, 0.35 mm, 0.24 mm, and 0.18 mm. The corresponding focal depths are 13.4 mm, 7.8 mm, 6.7 mm, and 4.4 mm. It can be concluded that the dark region and the focal depth of E_z gradually decrease with the frequency of the THz wave increasing. Additionally, the focusing ability of E_z for lenses with different NAs is also checked. Another Si lens with 50 mm focal length is used to focus the THz wave. The transverse and longitudinal distributions of the E_z components for 0.7 THz are presented in Figs. 4(e) and 4(f), respectively. The dark region and the focal depth of E_z are 0.43 mm and 20 mm, respectively. It shows that the focusing effect of E_z is weak with a smaller NA. These features are the same as those of the transverse component E_x.

IV. Final Abstract

In conclusion, the vector diffraction properties of a converging THz beam are systematically measured by using the THz digital holographic imaging system. Specially, the distribution of the E_z components of the focused THz beam with linear polarization is intuitively presented. The E_z component presents the dipole distribution. In addition, the theoretical expectations have also been given utilizing the Richards-Wolf formulas. The simulation results accurately reproduce the experimental phenomena. This work provides a solid experimental investigation of the diffraction properties of the electro-magnetic waves and demonstrates the ability of the THz digital holographic imaging system.

References

[1]. X. K. Wang, Y. Cui, W. F. Sun, J. S. Ye, and Y. Zhang, "Terahertz polarization real-time imaging based on balanced electro-optic detection," J. Opt. Soc. Am. A, 27, 2387-2393 (2010).
[2]. S. Winnerl, R. Hubrich, M. Mittendorff, H. Schneider, and M. Helm, "Universal phase relation between longitudinal and transverse fields observed in focused terahertz beams," New J. Phys., 14, 103049 (2012).
[3]. A. Boivin and E. Wolf, "Electromagnetic field in the neighborhood of the focus of a coherent beam," Phys. Rev., 138, 1561-1565 (1965).